Articles

NVP-DPP728 (1-[[[2-[(5-Cyanopyridin-2-yl)amino]ethyl]amino]acetyl]-2-cyano-(*S*)-pyrrolidine), a Slow-Binding Inhibitor of Dipeptidyl Peptidase IV

Thomas E. Hughes,* Manisha D. Mone, Mary E. Russell, Stephen C. Weldon, and Edwin B. Villhauer

Metabolic and Cardiovascular Diseases Research, Novartis Institute for Biomedical Research, 556 Morris Avenue, Summit, New Jersey 07901-1398

Received April 12, 1999; Revised Manuscript Received July 2, 1999

ABSTRACT: Inhibition of dipeptidyl peptidase IV (DPP-IV) has been proposed recently as a therapeutic approach to the treatment of type 2 diabetes. *N*-Substituted-glycyl-2-cyanopyrrolidide compounds, typified by NVP-DPP728 (1-[[[2-[(5-cyanopyridin-2-yl)amino]ethyl]amino]acetyl]-2-cyano-(*S*)-pyrrolidine), inhibit degradation of glucagon-like peptide-1 (GLP-1) and thereby potentiate insulin release in response to glucose-containing meals. In the present study NVP-DPP728 was found to inhibit human DPP-IV amidolytic activity with a K_i of 11 nM, a k_{on} value of 1.3×10^5 M^{-1} s^{-1}, and a k_{off} of 1.3×10^{-3} s^{-1}. Purified bovine kidney DPP-IV bound 1 mol/mol [^{14}C]-NVP-DPP728 with high affinity (12 nM K_d). The dissociation constant, k_{off}, was 1.0×10^{-3} and 1.6×10^{-3} s^{-1} in the presence of 0 and 200 μM H-Gly-Pro-AMC, respectively (dissociation $t_{1/2}$ ∼10 min). Through kinetic evaluation of DPP-IV inhibition by the D-antipode, des-cyano, and amide analogues of NVP-DPP728, it was determined that the nitrile functionality at the 2-pyrrolidine position is required, in the L-configuration, for maximal activity (K_i of 11 nM vs K_i values of 5.6 to >300 μM for the other analogues tested). Surprisingly, it was found that the D-antipode, despite being ∼500-fold less potent than NVP-DPP728, displayed identical dissociation kinetics (k_{off} of 1.5×10^{-3} s^{-1}). NVP-DPP728 inhibited DPP-IV in a manner consistent with a two-step inhibition mechanism. Taken together, these data suggest that NVP-DPP728 inhibits DPP-IV through formation of a novel, reversible, nitrile-dependent complex with transition state characteristics.

Dipeptidyl peptidase IV (DPP-IV, EC 3.4.14.5)[1] is a post-proline cleaving serine protease with significant sequence and structural similarity to other α-*β*-hydrolases (e.g., prolyl oligopeptidase, acetylcholinesterase). DPP-IV is found throughout the body, both circulating in plasma and as a type II membrane protein produced by a variety of tissues, including kidney, liver, and intestine. DPP-IV may play a role in cleavage and inactivation of biologically active peptides with accessible amino-terminal Xaa-Pro- or Xaa-Ala- sequences (*1, 2*). Indeed, DPP-IV degrades and regulates the activity of several regulatory peptides in man (including the gut peptide "incretin" hormone glucagon-like peptide-1 (GLP-1), growth hormone-releasing hormone, and gastric inhibitory polypeptide). Due to the impressive antidiabetic actions of GLP-1, DPP-IV inhibition has been proposed as an intriguing new approach to the therapy of type 2 diabetes mellitus (*3*).

Several classes of DPP-IV inhibitors bearing transition state mimics have been identified, and their kinetic properties have been extensively investigated. Peptidyl (α-aminoalkyl)-phosphate diphenyl ester inhibitors of DPP-IV bind with low affinity (10^{-4} M IC_{50} values) but rapidly form highly stable covalent complexes with the active site serine residue of DPP-IV (*4*). Pro-boroPro and related analogues bind with high affinity (K_i ∼10^{-11} M) in a reversible manner (half-life of enzyme−inhibitor complex ∼ 150 min; *5*). The boronic acid analogues, however, are unstable in solution due to reversible intramolecular cyclization, and also inhibit dipeptidyl peptidase II, a related serine protease. Irreversible "suicide substrate" methylsulfonio cyclopeptide inhibitors have been described (*6*) as mechanistic tools but may not be suitable for therapeutic use. Although a series of (*N*-hydroxyacyl amide) aminodicarboxylic acid pyrrolidides have been described, only relatively unselective inhibitors with micromolar potency have been prepared (*7*). Conformationally constrained fluoroolefin-containing peptidyl-hydroxylamine inhibitors also have been described (*8*), but isolation of enantiomerically pure compounds requires tedious separation of diastereomers. For these reasons, new chemical classes of selective and potent DPP-IV inhibitors are of interest and needed in order to evaluate the feasibility and efficacy of DPP-IV inhibition as a therapeutic approach.

Recently, DPP-IV inhibitors with 2-cyanopyrrolidide P1 substituents have been reported (*9*, *10*). These compounds

* Author for correspondence. Tel: 908-277-7336. Fax: 908-277-7728. E-mail: thomase.hughes@pharma.novartis.com.

[1] Abbreviations: NVP-DPP728, 1-[[[2-[(5-cyanopyridin-2-yl)amino]-ethyl]amino]acetyl]-2-cyano-(*S*)-pyrrolidine; DPP-IV, dipeptidyl peptidase IV; pNA, *p*-nitroaniline.

10.1021/bi990852f CCC: $18.00
Published on Web 08/18/1999

Chart 1. Structures of NVP-DPP728 and Analogs

NVP DPP728

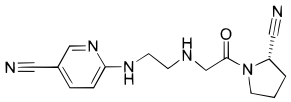

D-antipode

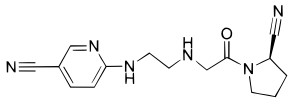

Des-cyano analog

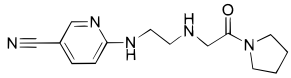

Amide analog

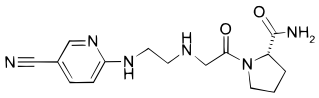

bind to DPP-IV several orders of magnitude more tightly than the corresponding pyrrolidide analogues (e.g., K_i values for isoleucine-2-cyanopyrrolidide and isoleucine pyrrolidide are 2 and 400 nM, respectively; *10*, *11*). Similar potency is observed with a new class of cyanopyrrolidide inhibitors, termed *N*-substituted-glycyl-2-cyanopyrrolidide compounds (*12*). Recently, NVP-DPP728 (see Chart 1), a novel derivative of this class, has been identified as a potent and selective DPP-IV inhibitor for use in the treatment of diabetes mellitus (example no. 5 in ref *12*, described also in ref *13*). NVP-DPP728 inhibits human and rat plasma DPP-IV with IC_{50} values in the range of 5−10 nM with >15 000-fold selectivity relative to DPP−II and a range of proline-cleaving proteases (*13*). This compound shows promise as an antidiabetic agent due to its ability to preserve the integrity of GLP-1 (*13*) and improve glucose tolerance (*14*).

While dipeptide-like pyrrolidide compounds (e.g., valine pyrrolidide) inhibit DPP-IV through simple reversible competitive binding (*11*), the kinetic properties of nitrile-containing inhibitors have not been rigorously evaluated. In a brief communication, Li and colleagues (*9*) reported that dipeptide cyanopyrrolidide compounds generate competitive or mixed inhibition profiles and postulated that the mechanism of inhibition involves formation of an imidate intermediate, (comparable to the thioimidate intermediate state known for nitrile−cysteine protease complexes; *15*, *16*).

We hypothesized that imidate formation for nitrile DPP-IV inhibitors, if analogous to cysteine protease inhibition, should display slow-binding inhibition kinetics. A series of studies, focused on NVP-DPP728, have been undertaken to define the kinetic and molecular mechanisms for responsible for the potent inhibition of DPP-IV by cyanopyrrolidine compounds. Here we report that NVP-DPP728 inhibits DPP-IV by a slow-binding mechanism and that the rate of inactivation is dependent upon L-chirality of the pyrrolidine nitrile functionality. The binding affinity and rate of dissociation of bound inhibitor determined by kinetic experiments were further confirmed by direct binding measurements using radiolabeled NVP-DPP728 and DPP-IV highly purified from bovine kidney cortex.

EXPERIMENTAL PROCEDURES

Materials. Bovine serum albumin, bromelain, calf intestinal adenosine deaminase, CNBr-activated Sepharose 4B, and *p*-nitroaniline were from Sigma (St. Louis, MO). H-Ala-Pro-pNA was from Bachem (King of Prussia, PA). Bovine kidney cortices were obtained from Pell Freeze Biological (Rogers, AR). The human colonic carcinoma cell line Caco-2 was obtained from the American Type Culture Collection (ATCC HTB 37).

Inhibitors. NVP-DPP728 was prepared as described (compound no. 5 in ref *12*). The D-antipode, des-cyano, and amide analogues of NVP-DPP728 were prepared as described (*13*). Dr. Tapan Ray (Novartis Radiosynthesis Laboratory), incorporating the label at the carbonyl carbon, kindly provided [^{14}C]-NVP-DPP728 (specific activity 49 mCi/mmol).

Preparation of Human and Bovine DPP-IV. Where indicated, human DPP-IV preparations consisted of extracts of Caco-2 cells (*17*), cultured as previously described to induce differentiation (*18*). Cell extract containing human DPP-IV was prepared from cells solubilized in 10 mM Tris-HCl, 0.15 M NaCl, 0.04 tiu aprotinin, 0.5% nonidet-P40, pH 8.0, by centrifugation at 35 000*g* for 30 min at 4 °C to remove cell debris. The preparations contained approximately 30 mU DPP-IV/mg (~0.6 μg/mg of protein; 1 unit cleaves 1 μmol of H-Ala-Pro-pNA/min; enzyme content derived from V_{max} determined using Gly-Pro-4-nitroaniline, using a theoretical maximal activity of 55 U/mg as described (*19*)). Bovine DPP-IV was purified from kidney cortex using adenosine deaminase (ADA) affinity chromatography as previously described (*20*). Following digestion of a microsomal membrane fraction with bromelain, the resulting soluble protein was resolved by sequential Q-Sepharose, ADA-Sepharose 4B, and Mono-Q chromatography to yield a >90% pure DPP-IV enzyme preparation with a molecular weight by SDS−PAGE of 105 kDa (specific activity was 20 units/mg of protein).

Kinetics of Inhibition of DPP-IV. The progress of DPP-IV inhibition by the indicated compounds was measured under pseudo-first-order inhibition conditions, i.e., $[I_0] \geq 10\text{-}[E_0]$, by reacting DPP-IV with a mixture of inhibitor and substrate and recording the liberation of free pNA at 405 nm. Unless otherwise indicated, all reactions were conducted using 20 μg of extract protein in 25 mM Tris-HCl, 140 mM NaCl, 10 mM KCl, 1% bovine serum albumin, pH 7.4, at 25 °C (referred to as "assay buffer"). Under these conditions, K_m for H-Ala-Pro-pNA was 73 μM. Reaction progress was monitored using a Molecular Devices SpectraMax Plus microplate spectrophotometer (Sunnyvale CA). Reactions were 0.15 mL of final volume, initiated by the addition of a 5 μL aliquot of enzyme stock and mixed using the automated mixing feature of the SpectraMax reader. Total elapsed time between enzyme addition and the initiation of data collection was less than 30 s. Readings were taken every 10 s for a total of 1000 s, and initial (blank) absorbance values were subtracted from the data prior to subsequent calculations. Data were exported to Microsoft Excel and subsequently into the data analysis package Origin (Microcal Software Inc., Northampton, MA) where curve fitting was performed. Data were fitted to the integrated rate equation for slow binding inhibition (eq 1) according to the method described by

$$A = v_s t + (v_0 - v_s)(1 - e^{-k't})/k' + A_0$$

Williams and Morrison (1979), by nonlinear regression analysis. Values for v_0 (initial rate), v_s (final steady-state rate),

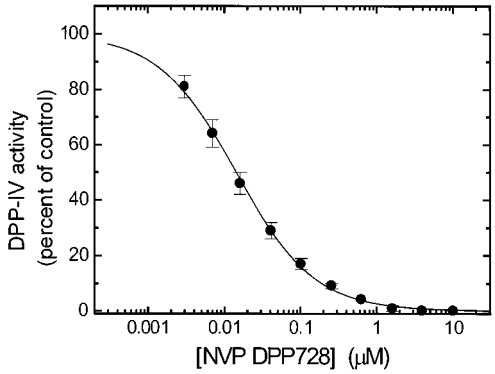

FIGURE 1: Dose−response curve of DPP-IV inhibition by NVP-DPP728. Following a 10-min preincubation of human DPP-IV with the indicated concentrations of inhibitor, the reaction was initiated by the addition of H-Ala-Pro-pNA (166 μM final concentration). Values are means ± SEM of three independent experiments. The line represents the logistic function with upper and lower asymptotes and slope fixed at 100, 0, and 1, respectively. The IC_{50} value derived from these data is 14 nM.

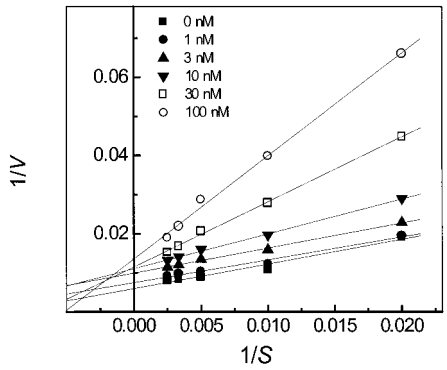

FIGURE 2: Lineweaver−Burk plot of DPP-IV activity measured in the presence of varied concentrations of NVP-DPP728 and substrate. Inhibitor effects were assessed as described in the legend to Figure 1, except both inhibitor and substrate concentrations were varied. Symbols correspond to different inhibitor concentrations as indicated in the legend. Values are means of triplicate determinations in which the standard deviations were less than 5% of the mean values. Lines shown are the least-squares linear regression lines.

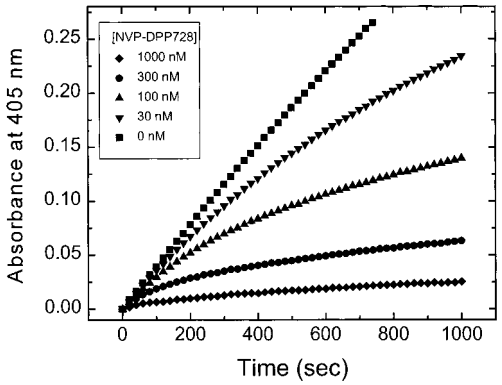

FIGURE 3: Slow-binding kinetics for the inhibition of DPP-IV by NVP-DPP728. Progress curves for pNA generation were recorded over 1000 s (16.7 min) at 405 nm. Measurement was done in 25 mM Tris-HCl pH 7.4, 140 mM NaCl, 10 mM KCl, and 1 wt %/vol bovine serum albumin in the presence of 166 μM H-Ala-Pro-pNA. Values are shown corrected for background absorbance (approximately 0.03 AU). Symbols correspond to different inhibitor concentrations as indicated in the legend. Values are from one of three replicate studies.

k' (apparent rate constant for the transition from v_0 to v_s), and A_0 (the initial absorbance at 405 nm) were obtained for each progress curve. These values were subsequently used to generate k_{on} (association rate constant), k_{off} (dissociation rate constant), and K_i values as described in the Results.

Radiolabeled Inhibitor Binding. Binding and dissociation of [^{14}C]-NVP-DPP728 were studied by incubating 2.5 μg (23 pmol) of purified bovine kidney DPP-IV with inhibitor in a volume of 4 mL of 50 mM Tris-HCl, pH 8.0, for 5 min at 25 °C, followed by capture on DEAE cellulose membrane disks (25 mm diameter, Schleicher & Schuell). Bound enzyme was rapidly washed with 1 mL of the same buffer at 4 °C, and both bound and eluted ^{14}C were quantified by liquid scintillation counting in a Beckman (Columbia, MD) LS6000IC scintillation counter with quench correction (counting time was 20 min or 2% of σ). Nonspecific binding, less than 10% of the total bound activity, was determined in the presence of a 1000-fold excess of nonradioactive NVP-DPP728. For determination of dissociation rates of the enzyme−inhibitor complex, bovine kidney DPP-IV was incubated (2.5 μg/time point) as above with 1000 nM [^{14}C]-NVP-DPP728 for 10 min, followed by capture with 100 μL of a 5:1 (gel:buffer) slurry of ADA-Sepharose 4B. The samples were then incubated with mixing for 20 min, and enzyme-bound inhibitor was collected on a 0.45 μm nylon-66 membrane (Rainin, Woburn MA). The resin (with immobilized labeled inhibitor) was resuspended in 10 mL of buffer ([EI] after dilution was 2.3 nM). At the indicated time points, samples were removed and quickly filtered through Whatman type 1 filter paper disks (2.5 cm). The trapped resin was rapidly washed with 1 mL of ice-cold assay buffer, and both trapped (enzyme bound) and eluted (free) inhibitor were quantified by scintillation counting. Blanks containing radiolabeled inhibitor, but no enzyme, were subtracted from both the bound and free counts and were less than 10% of the total radioactivity. Dissociation curves were plotted as the log of the fraction of initial bound enzyme versus time following dilution. Off-rates were calculated as the slope of these plots.

Inhibitor Stability. Under the conditions employed, NVP-DPP728 undergoes intramolecular cyclization, yielding a cyclic imidate product, with a half-life of approximately 72 h. Accordingly, less than 1% of the compound is expected to cyclize during the time frame of the current investigations.

RESULTS

NVP-DPP728 fully inhibited H-Ala-Pro-pNA cleavage by DPP-IV derived from human colonic adenocarcinoma cells with an IC_{50} value of 14 nM (Figure 1). NVP-DPP728 displayed complex inhibition kinetics when assessed graphically by Lineweaver−Burk analysis (shown for illustrative purposes in Figure 2), consistent with results reported (*9*) for Xaa-cyanopyrrolidide compounds. Assessment of reaction progress curves in the presence of varied inhibitor concentrations revealed a clear time-dependent approach to steady state, characteristic of slow binding inhibition kinetics (Figure 3). These progress curves were fitted to eq 1 to determine values for k_{on}', the association rate constant for inhibitor binding. Values for k' were plotted against the inhibitor concentration, [I_0] (Figure 4). A linear dependency between [I_0] and k' was observed and fitted (eq 2) to obtain estimates

Table 1: Kinetic Constants for DPP-IV Inhibition by Pyrrolidine Compounds[a]

compd	P1′ substituent[b] S	P1′ substituent[b] R	K_i (μM)	k_{on} (10^3 M^{-1} s^{-1})	k_{off} (s^{-1})	EI half-life (h)
NVP-DPP728	CN	H	0.011 ± 0.004	127 ± 27	(1.3 ± 0.2) × 10^{-3}	0.14
D-antipode	H	CN	5.6 ± 1.4	0.27 ± 0.03	(1.5 ± 0.2) × 10^{-3}	0.13
des-cyano	H	H	15.6 ± 3.6	rapid	rapid	<0.01
amide	$CONH_2$	H	320 ± 118	ND	ND	ND
Pro-boroPro[c]	$B(OH)_2$	H	0.000016	5000	0.078 × 10^{-3}	2.5
Pro-Pro$(OPh)_2$[d]	Pro$(OPh)_2$	H	70	0.02	irreversible	>672

[a] Reactions were performed at 25 °C in 25 mM Tris-HCl, pH 7.4, containing 140 mM NaCl, 10 mM KCl, 1% bovine serum albumin, and 166 μM H-Ala-Pro-pNA. Values are means ± standard deviations for three experiments. [b] Functional group present at the pyrrolidine-2-position. [c,d] Values are from Gutheil and Bachovchin (*5*) and from Lambeir et al. (*23*), respectively. ND: not determined. EI half-life values were calculated as the ratio of 0.693/k_{off}.

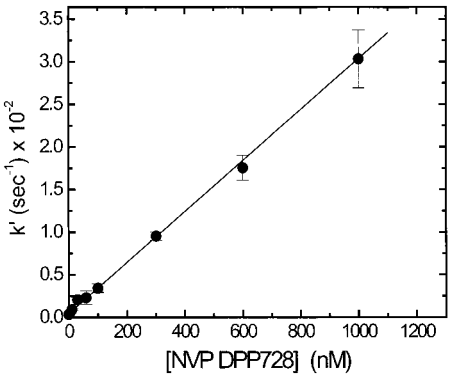

FIGURE 4: Determination of the association rate constant k_{on}' from a plot of k' vs $[I_o]$. The line represents a least squares linear fit of the indicated k' and I (NVP-DPP728 concentration) values. k' values were calculated according to eq 2. The line predicts a slope (k_{on}') of 0.47 μM^{-1} s^{-1}. Values are means ± SEM of three separate experiments.

$$k' = k_{off} + k_{on}'[I_0] \quad (2)$$

of k_{on}' and k_{off}. The rate constant k_{on}' was subsequently corrected for the competition of the substrate using eq 3,

$$k_{on} = k_{on}'(1 + [S_0]/K_m) \quad (3)$$

where $[S_0]$ is the concentration of the chromogenic substrate and K_m is the separately determined Michaelis−Menton constant. K_i' values were determined using a direct, nonlinearizing plot of v_s vs I, fitted to eq 4.

$$v_s = v_0/(([I_0]/K_i') + 1) \quad (4)$$

K_i was subsequently calculated from K_i' according to eq 5.

$$K_i = K_i'/(1 + [S_0]/K_m) \quad (5)$$

The inhibition constants for NVP-DPP728, its D-antipode, and its des-cyano and amide analogues, determined in three separate experiments, are shown in Table 1. Potency of NVP-DPP728 was strongly dependent upon the presence and chirality of the P1 nitrile functionality. By alteration of the orientation (L- to D-) of the nitrile−pyrrolidine bond, approximately 500-fold loss of potency was observed. By removal of the nitrile substituent altogether (hydrogen replacement), a 1000-fold loss of potency resulted.

Similarly, placement of a more bulky amide substituent with substantially less dipole character in place of the nitrile resulted in a 30 000-fold loss of potency. These results

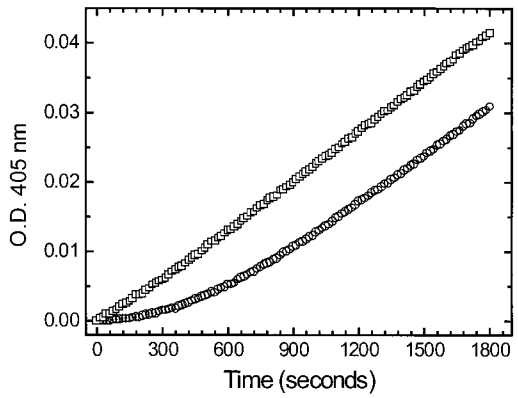

FIGURE 5: Dissociation of the NVP-DPP728−DPP-IV complex following dilution into substrate. An aliquot of DPP-IV enzyme previously incubated in the presence of 0 (squares) or 300 (circles) nM L-NVP-DPP728 was diluted 100-fold into 1 mM H-Ala-Pro-pNA, in assay buffer. Dissociation was monitored by substrate hydrolysis (absorbance at 405 nm). Absorbance readings were taken every 15 s for 30 min.

indicated that the nitrile functionality, in the L- (or S-) configuration, imparts approximately 3.9 kcal/mol of binding energy compared to the des-cyano (−H) analogue.

Inhibitor dissociation was studied by diluting the preformed NVP-DPP728/DPP-IV complex into a concentrated substrate solution such that the complex concentration was approximately 150-fold less than K_i' and the S/K_m ratio was >10. Figure 5 shows that the DPP-IV enzymatic activity was slowly recovered from the inhibitory complex, indicated by the nonlinear increase in rate relative to the control curve.

A value for k' was determined from the upwardly concave curve by fitting the data to eq 1, in which k' represents the rate for reestablishment of the steady-state equilibrium between DPP-IV and NVP-DPP728/DPP-IV complexes following dilution. A value for k_{-2} (Table 2, 1.4 ± 0.5 × 10^{-3} s^{-1}) was then derived by linear regression from a plot of k' against I (not shown), where the *y*-intercept is taken as the rate constant for decay of the NVP-DPP728/DPP-IV complex, as described (*22*). Comparison of disassociation rates calculated for the des-cyano analogue of NVP-DPP728 and the amide analogue (Table 1) indicate that the presence of the nitrile functionality of NVP-DPP728 imparts potency by promoting formation of a relatively long-lived complex.

Equilibrium binding experiments were carried out using [^{14}C]-labeled NVP-DPP728 in order to confirm the results obtained by kinetic methods and to assess the potential for effects of substrate on enzyme−inhibitor dissociation. The compound was bound to bovine kidney DPP-IV, and EI

Table 2: NVP-DPP728 Affinity and Dissociation Constants Determined by Kinetic and Binding Methods

method	$[S_0]$ (μM)	K_i (nM)	k_{off} (s^{-1})
Kinetic Methods			
initiated by enzyme addition[a]	166	11 ± 4	$(1.3 \pm 0.2) \times 10^{-3}$
	1000	15 ± 1	$(1.5 \pm 0.3) \times 10^{-3}$
initiated by dilution of EI[b]	166	16 ± 4	$(1.5 \pm 0.5) \times 10^{-3}$
Binding[c] Methods			
without substrate	0	12 ± 2	$(1.0 \pm 0.1) \times 10^{-3}$
with substrate	200	ND	$(1.6 \pm 0.1) \times 10^{-3}$ [c]

[a] Reactions were initiated by the addition of enzyme and were performed at 25 °C in 25 mM Tris-HCl, pH 7.4, containing 140 mM NaCl, 10 mM KCl, 1% bovine serum albumin, and H-Ala-Pro-pNA as indicated. [b] Reactions were initiated by 100-fold dilution of enzyme preincubated for 60 min with NVP-DPP728 into buffer containing substrate. Inhibition constants were determined as described in the Results. [c] Binding and dissociation of [^{14}C]-NVP-DPP728 to purified bovine kidney DPP-IV was measured at 25 °C in 50 mM Tris-HCl, pH 8.0, and 150 mM NaCl. Following washing of DPP-IV saturated with [^{14}C]-NVP-DPP728 and dilution into buffer containing 0 or 200 μM Gly-Pro-AMC, bound and free inhibitor were collected by filtration and quantitated by scintillation counting. [c] Significantly different from 0 substrate value ($p < 0.0001$ by Student's t test). ND: not determined.

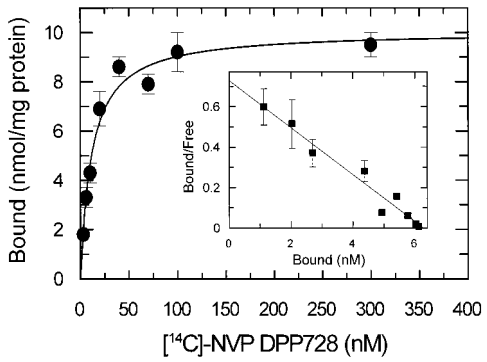

FIGURE 6: Equilibrium binding of [^{14}C]-NVP-DPP728 to bovine kidney DPP-IV. Aliquots (2.5 μg) of bovine DPP-IV were diluted into 50 mM Tris-HCl, pH 8.0, containing 0−300 nM [^{14}C]-NVP-DPP728. Following a 10-min incubation, enzyme-bound inhibitor was separated from free inhibitor and quantified by scintillation counting. The data represent the mean (SEM) of three independent experiments.

complexes were adsorbed onto DEAE cellulose disks. After subtraction of nonspecific binding, the data were fit (Figure 6) according to eq 6, where [EI] is the concentration of

$$[EI] = [E_{total}][I]/(K_d + [I]) \quad (6)$$

enzyme−inhibitor complex, [I] is the free inhibitor concentration, $[E_{total}]$ is the enzyme concentration, and K_d is the dissociation constant (equivalent to K_i).

The calculated K_d and $[E_{total}]$ derived from these data were 11.5 ± 1.8 nM and 10.0 ± 0.4 nmol/mg of protein, respectively. On the basis of a unit molecular weight of 110 000 Da, approximately 1 mol of binding was observed per mol of enzyme. The data also were plotted according to the method of Scatchard (*24*) (see eq 7, inset to Figure 6),

$$[EI]/[I] = ([EI]_{max} - [EI])/K_d \quad (7)$$

where the slope of the fit line is equal to $1/K_d$ and the x-intercept is equal to $[EI]_{max}$. The K_d value obtained by this method was 8.6 nM, in agreement with the value obtained by both the saturation binding and kinetic methods. The x-intercept (6.3 nM), equal to the concentration of binding sites, agreed well with the enzyme concentration of 5.7 nM. Thus, using equilibrium binding measurements with radiolabeled compound, it was possible to confirm the affinity measurements obtained using kinetic methods and to substantiate a model for single-site, competitive binding.

Scheme 1

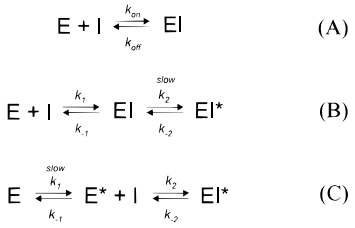

Since the both the D-antipode and the des-cyano analogue of NVP-DPP728 were found to have similar, low potency (K_i values of 5.6 and 15.6 μM, respectively), it appeared that L-chirality was required for high-affinity binding of the nitrile functionality. Surprisingly, evaluation of the inhibition kinetics for the D-antipode revealed essentially identical dissociation rates (k_{off} values of 1.5 and 1.3×10^{-3} s^{-1} for the D- and L-isomers, respectively). Because the pair of inhibitors bind with markedly different association rates (127×10^3 vs 0.27×10^3 M^{-1} s^{-1}), but dissociate with identical kinetics, a series of experiments were performed to dissect the mechanism of slow binding.

As described above, reaction progress curves obtained in the presence of a range of inhibitor concentrations indicated that NVP-DPP728 obeyed slow-binding inhibition kinetics. This behavior was indicated by the observation that NVP-DPP728-mediated inhibition of H-Ala-Pro-pNA cleavage approached steady-state equilibrium on a time scale of minutes under the conditions employed and the data could be fitted robustly to the slow-binding equation (*22*). Three mechanisms have been proposed that describe slow-binding behavior (Scheme 1, after Cha (*25*)).

In mechanism A, enzyme (E) binds to the inhibitor (I) in a slow step to form a tight EI complex. In mechanism B, a loose EI complex forms rapidly and is followed by a (relatively) slow isomerization to a tight EI* complex. Mechanism C describes a slow isomerization of free enzyme (E) to form E* which can rapidly and tightly bind I, forming a tight EI* complex. To discriminate between the binding mechanisms, the relationships observed between I and k′, and between I and v_0, were assessed. The initial velocity (v_0) was found to be significantly inhibited in proportion to the inhibitor concentration (Figure 7) for NVP-DPP728, a finding inconsistent with mechanism A in which v_0 is predicted to be unaffected by the concentration of inhibitor (*22*).

The observation that the first-order rate constant k' increased with increasing inhibitor concentration (illustrated in Figure 4) was consistent with mechanisms A and B but not mechanism C, in which k' should decline with increasing inhibitor concentration. For this reason, mechanism B appears to best explain inhibition of DPP-IV by NVP-DPP728.

Dissociation studies employing radiolabeled NVP-DPP728 were conducted with purified bovine DPP-IV to confirm the binding constants determined by kinetic means using DPP-IV contained in cell extracts. For these studies, purified

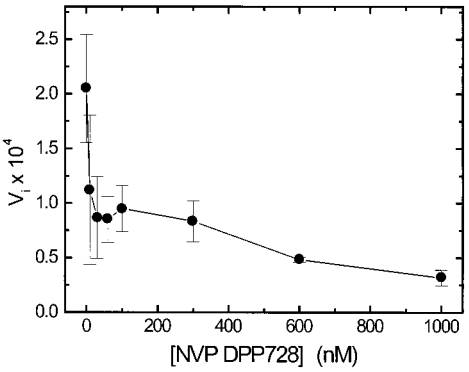

FIGURE 7: Dependence of initial velocities (v_0) on NVP-DPP728 concentration. Data represent initial velocity (v_i) values derived using eq 1 from progress curves measured as described in Figure 3. Measurement was done in 25 mM Tris-HCl pH 7.4, 140 mM NaCl, 10 mM KCl, and 1 wt %/vol bovine serum albumin in the presence of 1 mM H-Ala-Pro-pNA. Values shown are means (SEM) of three experiments.

bovine kidney DPP-IV was saturated with [^{14}C]-labeled NVP-DPP728, trapped with ADA-Sepharose, washed, and resuspended in buffer (with or without 0.2 mM H-Gly-Pro-AMC) such that the concentrations of enzyme and inhibitor were $\leq 0.2\ K_i$. The concentrations of free and bound inhibitor were determined at 0, 1, 2, 3, 4, 6, 8, and 10 min after resuspension in buffer. The data (percent bound vs time) were fitted to a single-exponential decay curve (eq 8), where [EI],

$$[EI] = [EI]_0 e^{-kt} \quad (8)$$

$[EI]_0$, and k are the concentration of enzyme−inhibitor complex at time t, the concentration of complex at time 0, and the rate constant, respectively. The half-life for inhibitor dissociation was taken as the natural log of 2 (0.693) divided by the rate constant and was determined to be 11.9 and 7.2 min in the absence and presence of substrate, respectively ($p < 0.0001$ by Student's t test, Table 2). These results indicated that, although the effects were relatively minor and although the dissociation of the inhibitor from the enzyme−inhibitor complex occurred more rapidly in the presence of the dipeptide substrate than in its absence, the enzymatically determined kinetic results represented a reasonable prediction of dissociation kinetics.

DISCUSSION

We have identified a new class of potent cyanopyrrolidine inhibitors in which a glycyl Xaa amine moiety is substituted with aliphatic and aromatic substituents (*12*, *13*). These inhibitors are remarkably specific for inhibition of DPP-IV relative to other post-proline and -alanine cleaving enzymes (e.g., prolyl oligopeptidase, aminopeptidase P, and DPP-II). We have assessed kinetic behavior of this series in detail, focusing in this report on NVP-DPP728.

Through kinetic evaluation of DPP-IV inhibition by NVP-DPP728, as well as by direct measurement of radiolabeled inhibitor binding in the presence and absence of substrate, we have established that NVP-DPP728 derives its potency through a slow-binding inhibition mechanism. Formation of the high-affinity complex is dependent upon the nitrile functionality within this series. Substitution with a variety of other substituents (e.g., amide, hydrogen) is associated with a significant loss of inhibitory potency as well as a clear loss of time-dependent function. Interestingly, while moving the nitrile from the L- to the D-configuration substantially reduces the overall potency of the compound, this loss of potency is due to a ~500-fold slower binding rate (k_{on}, Table 1). Indeed, the dissociation kinetics for the L- and D-enantiomers are identical, indicating that once formed, reversal of the high-affinity complex is independent of the nitrile orientation.

Scheme 2. Proposed Model for Inhibition of DPP-IV by NVP-DPP728

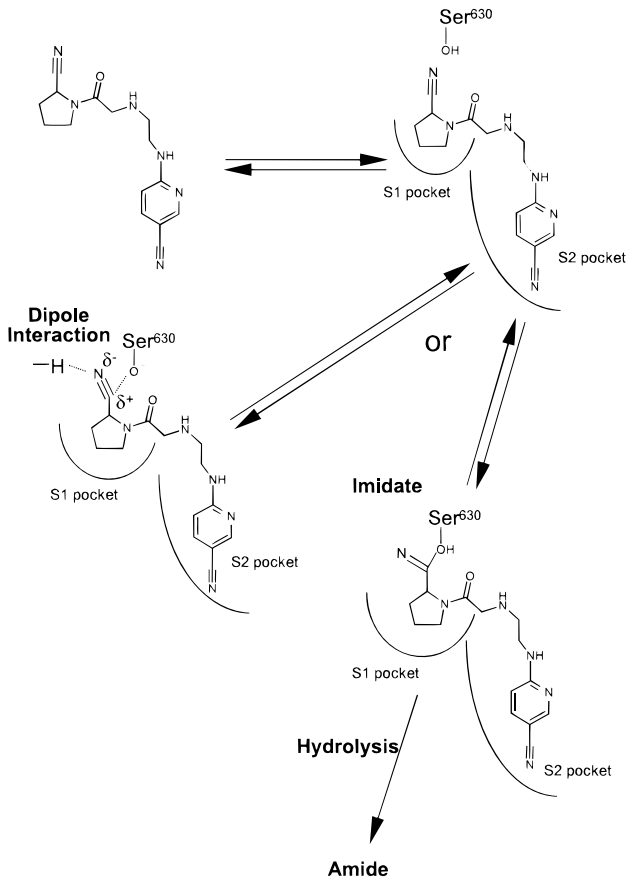

While it is not presently possible to precisely determine the mechanism of binding of NVP-DPP728 to DPP-IV, structure−activity relationships support the involvement of several key interactions. First, the pyrrolidide ring interacts with the S1 pocket, through van der Waals or hydrophobic interactions. Second, hydrogen-bonding and ionic interactions stabilize the peptide bond carbonyl and the P2 site basic nitrogen functionality, respectively. Third, hydrophobic interactions stabilize P2 site side-chain binding in the S2 pocket. These interactions may occur equally with nitrile and non-nitrile inhibitors. The negative charge derived from the acid−base−nucleophile (Asp-His-Ser) charge relay in the vicinity of the nitrile carbon drives a dipole−hydrogen bond interaction (interactions with both a hydrogen bond donor and the negatively charged active site serine) or transient imidate intermediate. The free energy change associated with the nitrile functionality, approximately 3.9 kcal/mol, may be adequately explained by either approach. These alternative high affinity state models are depicted in Scheme 2.

Although additional and novel inhibition mechanisms can potentially be forwarded, several consequences of the model shown in Scheme 2 can be feasibly approached and will be

addressed in subsequent communications. First, formation of an imidate intermediate should frequently proceed via hydration to yield a transformed amide byproduct (as observed for nitrile cysteine protease inhibitors; *26*). A hydrogen-bond-stabilized dipole interaction would, in contrast, be readily reversible, and inhibitor dissociation should generate unchanged parent compound only. Second, it should be possible to identify, through site-directed mutagenesis or through X-ray crystallography, the involvement of residues acting as hydrogen bond donors, capable of stabilizing nitrile inhibitor interactions. Recently, a high-resolution X-ray crystallographic structure of prolyl oligopeptidase has been reported (*27*) in which a tyrosine hydroxyl residue has been demonstrated to participate in stabilization of the oxyanion intermediate formed during binding of Z-pro-prolinaldehyde, a highly potent slow-binding inhibitor. Prolyl oligopeptidase is a member of the α,β-hydrolase family, closely related to DPP-IV. The observation that hydrogen-bonding interactions may contribute to the stabilization of catalytic intermediates could potentially extrapolate to DPP-IV. Indeed, the finding that DPP-IV and prolyl oligopeptidase (*28*), both serine proteases, are strongly inhibited by nitrile-based inhibitors indicates that significant mechanistic differences may emerge which distinguish DPP-IV and other α,β-hydrolase enzymes from the major classes of serine proteases.

As an agent under consideration for therapeutic utility in the management of a chronic disease (type 2 diabetes mellitus), NVP-DPP728 offers high potency, competitive behavior, and rapid reversibility. Since the long-term safety and side-effect profile of DPP-IV inhibitors has not been established in the human population, particularly with regard to inhibitor effects on peptide substrates other than GLP-1, compounds with rapid reversibility may have a safety advantage due to the ability of DPP-IV activity to recover on a daily basis. This may be of particular importance with regard to inhibitor effects on natural peptide substrates other than GLP-1 including growth hormone-releasing hormone (*2*) glucagon-like peptide-2 (29) and neuropeptides such as Substance P (*30*). Use of NVP-DPP728 as an antidiabetic agent is predicated on the therapeutic effects of glucagon-like peptide-1 (GLP-1), a small peptide hormone produced by the intestine during the absorption of nutrients. GLP-1, with a His-Ala- amino terminus, is rapidly cleaved and inactivated by DPP-IV (*2, 31*). By preserving GLP-1 activity in circulation, DPP-IV inhibitors are expected to improve insulin release following ingestion of meals, to suppress glucagon, a stimulus for hepatic glucose production, and to augment satiety (*3*). Thus rapidly reversible inhibitors that inhibit GLP-1 degradation, which are present during meal absorption and which are readily cleared from circulation, will exert a therapeutic effect while allowing other DPP-IV-mediated functions to be minimally affected. As an inhibitor with high potency and rapidly reversible inhibition kinetics, NVP-DPP728 will allow for the safety and tolerability of DPP-IV inhibition to be evaluated under conditions allowing intermittent recovery of enzyme function.

ACKNOWLEDGMENT

The excellent technical assistance of John Brinkman and Goli Naderi is kindly acknowledged. We are indebted to Dr. Ulf Neumann (Novartis Pharma Ltd.) for helpful input during preparation of the manuscript.

REFERENCES

1. Yaron, A., and Naider, F. (1993) *Crit. Rev. Biochem. Mol. Biol. 28*, 31−81.
2. Mentlein, R., Gallwitz, B., and Schmidt, W. E. (1993) *Eur. J. Biochem. 214*, 829−835.
3. Holst, J. J., and Deacon, C. F. (1998) *Diabetes 47*, 1663−1670.
4. Boduszek, B., Oleksyszyn, J., Kam, C.-M., Selzler, J., Smith, R. E., and Powers, J. C. (1994) *J. Med. Chem. 37*, 3969−3976.
5. Gutheil, W. G., and Bachovchin, W. W. (1993) *Biochemistry 32*, 8723−8731.
6. Nguyen, C., Blanco, J., Mazaleyrat, J. P., Krust, B., Callebalut, C., Jacotot, E., Hovanessian, A. G., and Wakselman, M. (1998) *J. Med. Chem. 41*, 2100−2110.
7. Demuth, H.-U., Schlenzig, D., Schierhorn, A., Grosche, G., Chapt-Chartier, M.-P., and Gripon, J.-C. (1993) *FEBS Lett. 320*, 23−27.
8. Lin, J., Toscano, P. J., and Welch, J. T. (1998) *Proc. Natl. Acad. Sci. U.S.A. 95*, 14020−14024.
9. Li, J., Wilk, E., and Wilk, S. (1995) *Arch. Biochem. Biophys. 323*, 148−152.
10. Ashworth, D. A., Atrash, B., Baker, G. R., Baxter, A. J., Jenkins, P. D., Jones, D. M., and Szelke, M. (1996) *Bioorg. Med. Chem. Lett. 6*, 1163−1166.
11. Schön, E., Born, I., Demuth, H.-U., Faust, J., Neubert, K., Steinmetzer, T., Barth, A., and Ansorge, S. (1991) *Biol. Chem. Hoppe-Seyler 372*, 305−311.
12. Villauer, E. B. (1998) World Patent Application WO 98/19998.
13. Hughes, T. E., Balkan, B., and Villhauer, E. B. (1999) *Diabetes 48* (Supplement 1), A21.
14. Balkan, B., Kwasnik, L., Miserendino, R., Holst, J. J., and Li, X. (1999) Manuscript submitted to *Diabetologia*.
15. Liang, T.-C., and Abeles, R. H. (1987) *Arch. Biochem. Biophys. 252*, 626−634.
16. Moon, J. B., Colman, R. S., and Hanzlik, R. P. (1986) *J. Am. Chem. Soc. 108*, 1350−1351.
17. Darmoul, D., Lacasa, M., Baricault, L., Marguet, D., Sapin, C., Trotot, P., Barbat, A., and Trugman, G. (1992) *J. Biol. Chem. 267*, 4824−4833.
18. Reisher, S. R., Hughes, T. E., Ordovas, J. M., Schaefer, E. J., and Feinstein, S. I. (1993) *Proc. Natl. Acad. Sci. U.S.A. 90*, 5757−5761.
19. Demuth, H.-U., Neumann, U., and Barth, A. (1989) *J. Enzyme Inhib. 2*, 239−248.
20. DeMeester, I., Vanhoof, G., Lambeir, A. M., and Scharpe, S. (1996) *J. Immunol. Methods 189*, 99−105.
21. Williams, J. W., and Morrison, J. F. (1979) *Methods Enzymol. 63*, 437−467.
22. Morrison, J. F., and Walsh, C. T. (1988) *Adv. Enzymol. 61*, 201−301.
23. Lambeir, A. M., Borloo, M., De Meester, I., Belyaev, A., Augustyns, K., Hendriks, D., Scharpe, S., and Haemers, A. (1996) *Biochim. Biophys. Acta 1290*, 76−82.
24. Scatchard, G. (1949). *Ann. N.Y. Acad. Sci. 51*, 660−672.
25. Cha, S. (1975) *Biochem. Pharmacol. 24*, 2177−2185.
26. Gour-Salin, B. J., Storer, A. C., Castelhano A., Krantz, A., and Robinson, V. (1991) *Enzyme Microb. Technol. 13*, 408−411.
27. Fulop, V., Bocskei, Z, and Polgar, L. (1998) *Cell 94*, 161−170.
28. Arai, H., Nishioka, H., Niwa, S., Yamanaka, T., Tanaka, Y., Yoshinaga, K., Kobayashi, N., Miura, N., and Ikeda, Y. (1993) *Chem. Pharm. Bull. 41*, 1583−1588.
29. Drucker, D. J., Shi, Q., Crivici, A., Sumner-Smith, M., Tavares, W., Hill, M., DeForest, L., Coope, S., and Brubaker, P. L. (1997) *Nat. Biotech. 15*, 673−677.
30. Kikuchi, M., Fukuyama, K., and Epstein, W. L. (1988) *Arch. Biochem. Biophys. 26*, 369−376.
31. Deacon, C. F., Johnsen, A. H., and Holst, J. J. (1995) *J. Clin. Endocrinol. Metab. 80*, 952−957.

BI990852F